Automated and Comprehensive Quality Assessment of Nationwide Aerial LiDAR Data: Insights from the LiDAR-ITA Project

Vittorio Marco Casella, Marica Franzini, Davide Lodigiani

Dept. of Civil Engineering and Architecture, University of Pavia, Pavia, Italy - (vittorio.casella, marica.franzini, davide.lodigiani)@unipv.it

Keywords: LiDAR, Quality Assessment, Automated Validation, Plano-altimetric Accuracy, Congruency, Large-scale datasets.

Abstract

National LiDAR programs are increasingly adopted worldwide to support land management, infrastructure planning, and environmental monitoring. Italy launched its most extensive airborne LiDAR operation in July 2025 as part of the Integrated Monitoring System (SIM) project, funded by the National Recovery and Resilience Plan (PNRR). This effort represents the most extensive airborne LiDAR campaign ever conducted in the country, covering over 302,000 km^2, including coastal zones and major islands. The acquisition plan is designed to ensure a minimum point density of 10 points/m^2 and produce high-resolution DTMs and DSMs at a 0.25 m grid spacing. Given the unprecedented spatial and data volume, a robust, standardised, and fully automated quality assurance framework is essential. This paper presents the methodology used to evaluate geometric consistency and spatial accuracy across the national dataset. Congruence between overlapping flight strips is assessed by automatically extracting 100 × 100 m patches at regular intervals and computing point-to-point distances and cross-section profiles to detect horizontal and vertical discrepancies. Plano-altimetric accuracy is further evaluated through comparisons with terrestrial laser scanning (TLS) data collected in dedicated control areas, where robust plane fitting enables rigorous three-dimensional error estimation. Results from two control areas acquired with different sensors demonstrate the robustness and scalability of the proposed automated framework. The presented approach provides a reliable foundation for delivering high-precision national LiDAR products and offers a framework applicable to future large-scale geospatial acquisition programs.

1. Introduction

National LiDAR acquisition campaigns are large-scale aerial operations organized by governmental or state agencies to collect high-resolution three-dimensional data of terrain and surface features. These initiatives aim to generate detailed models of topography and vegetation that support land management, infrastructure planning, natural hazard assessment, and environmental monitoring.

Over the past decade, several countries have launched nationwide LiDAR programs to provide consistent, high-quality elevation data across their territories. In the United States, for example, the 3D Elevation Program (3DEP) provides nationwide coverage to support applications ranging from agriculture and engineering to disaster management (Scott et al., 2022). Similar initiatives have been implemented across Europe, including France and Germany, where national LiDAR acquisitions have been used to update cartographic products and improve hydrogeological analyses (Hopfstock et al., 2022).

France (Institut national de l’information géographique et forestière (IGN), 2026) provides a particularly relevant example in the European context, given the structural similarities between its national LiDAR initiative and the Italian project. Through its national mapping agency, the Institut National de l’Information Géographique et Forestière (IGN), France launched the LiDAR HD program, an ambitious multi-year campaign designed to acquire LiDAR data at a density of 10 points/m^2 across the entire national territory. Initiated in 2021, the program aims to produce a seamless, high-precision three-dimensional digital representation of France, covering approximately 550,000 km^2, by 2026. The IGN coordinates a consortium of private aerial operators together with its internal acquisition capabilities, deploying advanced hybrid sensor systems such as the Riegl VQ series, Leica TerrainMapper and CityMapper. These instruments belong to the same class of airborne LiDAR sensors, and, in several cases, are identical models to those employed in the present project, ensuring comparable acquisition characteristics in terms of point density, accuracy, and operational performance. To ensure geometric consistency across acquisitions conducted by multiple operators and sensor platforms, quality assurance procedures are centralized at IGN.

The first nationwide LiDAR survey in Italy was launched by the Ministry of Environment and Energy Security (MASE) on April 2025, as part of the Integrated Monitoring System (SIM) project funded by the National Recovery and Resilience Plan (PNRR). This campaign represents the most extensive airborne LiDAR operation ever conducted in the country, covering the entire national territory, including coastal zones and major river systems, for a total area exceeding 302,000 km^2. The initiative aims to acquire high-resolution digital terrain and surface models through advanced LiDAR technology combined with aerogravimetric measurements. These data will provide a robust foundation for hydraulic modelling, flood risk mapping, shoreline monitoring, and slope stability analysis, supporting strategic objectives in land management and environmental protection.

Ensuring the reliability and consistency of such extensive LiDAR datasets requires a robust, standardized quality-assurance framework that integrates automated procedures (Franzini et al., 2023). Given the unprecedented spatial coverage and data volume of the Italian national survey, relying solely on manual inspection would be impractical, time-consuming, and inherently prone to operator inconsistencies. Consequently, the adoption of algorithm-driven validation workflows becomes essential for systematically assessing data quality at the national scale.

These automated procedures are designed to identify potential anomalies in the Airborne Laser Scanning (ALS) dataset, including point density, elevation accuracy, and geometric

https://doi.org/10.5194/isprs-archives-XLIX-B2-2026-125-2026

congruency between adjacent flight strips. By analysing the statistical properties of point clouds and comparing them against predefined quality thresholds, automated systems can efficiently detect irregularities such as local density gaps, vertical offsets, or inconsistencies arising from sensor calibration issues or flight trajectory errors. Automation not only significantly accelerates the assessment process but also enhances reproducibility. Standardised algorithmic workflows ensure that the same validation criteria are consistently applied across the entire dataset, reducing subjectivity and minimizing the risk of human error. Moreover, scalable automated frameworks allow quality assessment procedures to be applied efficiently to continuously expanding databases, making them particularly suitable for national or continental LiDAR programs where datasets may cover hundreds of thousands of square kilometres and contain billions of points.

1.1 Characteristics of LiDAR-ITA Project

The Italian national LiDAR survey, launched under the National Recovery and Resilience Plan (PNRR), represents the most extensive airborne LiDAR campaign ever conducted in the country, covering over 302,000 km^2, including all mainland areas and major and minor islands. The campaign started in April 2025 and is scheduled to be completed by June 2026, providing a homogeneous, high-quality LiDAR dataset to support national-scale applications in hydrology, geomorphology, risk assessment, and environmental management.
The airborne LiDAR surveys are conducted by two aerial survey companies, Compagnia Generale Ripreseaeree (CGR) and Italian Remote Sensing (I-R-S), using a fleet of 11 aircraft equipped with state-of-the-art LiDAR sensors. For most of the territory, conventional linear-mode LiDAR sensors, such as the Leica TerrainMapper (Leica, 2019), RIEGL VQ-1460 (RIEGL, 2026a), and VQ780 II-S (RIEGL, 2026b), capable of up to 2 MHz, will be employed. These sensors can record at least four returns per pulse, enabling detailed characterisation of terrain and vegetation structure, including canopy layers, understory, and subtle topographic variations. Even in complex environments, such as rugged landscapes, the multi-echo capability allows the laser pulses to penetrate vegetation and reach the ground, providing accurate measurements of both the surface and underlying terrain. This capability supports the generation of high-resolution digital terrain models (DTMs) and digital surface models (DSMs), and is particularly valuable for applications in geomorphology, forestry, hydrology, and habitat mapping. In contrast, a single-photon LiDAR (SPL) sensor, the Leica SPL100 (Brown et al., 2020), operating at up to 6 MHz, will be used in complex alpine regions. This sensor can detect individual photons in the returned laser signal, enabling rapid acquisition over complex terrain even at higher flight altitudes and generating high-density point clouds. Its high sensitivity and efficiency make it particularly suitable for large-scale topographic mapping in challenging environments.
As the Italian territory is characterised by a complex topography, including the Alpine and Apennine mountain regions, flight planning at the national scale must account for significant terrain variability. Flight planning is optimised to ensure full coverage, with overlapping strips and adaptive altitude to maintain point density even in complex topography. The acquisition plan is designed to ensure a minimum point density of 10 points/m^2, uniformly across plains, hills, and mountain regions, exceeding the original requirements of 8 points/m^2 in lowlands and 6 points/m^2 in mountainous areas.
Raw LiDAR data processing is performed by the same airborne survey companies (CGR and I-R-S) that conducted the LiDAR acquisitions, while the final products are processed by MERMEC Engineering. This approach ensures seamless integration of acquisition and processing workflows, leveraging the company’s specialized expertise, software, and well-established quality-control procedures. At a national-scale survey, the sheer volume of raw data produced is substantial, reaching hundreds of terabytes. These companies are equipped with high-performance computing infrastructure and extensive storage capacities, enabling them to efficiently manage the extremely large datasets generated during national-scale surveys.
The dataset resulting from the LiDAR flights will provide a comprehensive set of derived LiDAR products for the entire surveyed area, such as:

- Classified point clouds: tiled point clouds derived from a 1 × 1 km² tiling scheme, classified into ground and non-ground points, with outliers identified and flagged.
- Digital Terrain Models (DTMs) and Digital Surface Models (DSMs): high-resolution surface models, generated with a grid spacing of 0.25x0.25 m^2.

All datasets are referenced to the ETRF2000 coordinate system (epoch 2008.0), using EPSG:7794 for projected (cartographic) coordinates and EPSG:6706 for geographic coordinates. To ensure the dataset's reliability, rigorous calibration and quality control procedures are implemented, including the use of 70 distributed ground control areas and systematic validation against GNSS-surveyed checkpoints. According to the acquisition tender, the positional accuracy is expected to be better than 15 cm horizontally and 8 cm vertically, verified on open, flat terrain.

1.2 Control areas and the ALS dataset

The project is ongoing, with data acquisition and processing underway. Two test areas have been selected to evaluate raw LiDAR data, serving as pilot sites to validate verification procedures and test the LiDAR sensors that will be used to survey the entire Italian territory. At this stage, the complete dataset is not yet available for publication. The areas have been defined as approximately 2,500 square km in size, located in northern and central Italy, and acquired by two different LiDAR sensors owned by two different companies (Figure 1).

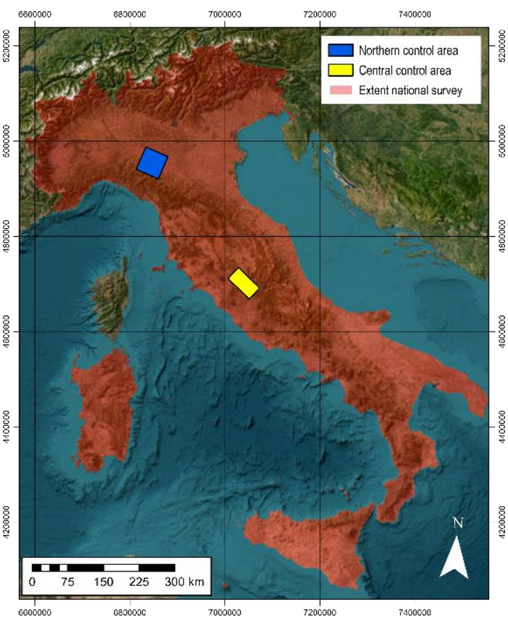

Figure 1. Map of the LiDAR survey area showing the control sites. The blue polygon indicates the northern control site, while the yellow polygon represents the southern control site (CRS: ETRF2000, epoch 2008.0, EPSG:7794).

https://doi.org/10.5194/isprs-archives-XLIX-B2-2026-125-2026

The first study area, referred to as the Northern test site, covering approximately 2,597 km^2, is in the Emilia-Romagna region and encompasses part of the Apennines. This area presents a highly diverse landscape, ranging from urban settlements to mountainous terrains, and includes both natural and semi-natural environments. Such variability enables testing and validation of LiDAR data acquisition and processing across diverse topographic and environmental conditions. The second study area, referred to as the Central test site, covering approximately 1,985 km^2, is situated in the Lazio region and similarly includes a portion of the Apennines, ensuring that the study encompasses a representative mix of Italian terrains, from urban centers to complex mountainous regions.

Both control areas were deliberately selected to capture the heterogeneity of the Italian territory. Each site combines mountain and urban environments, making it suitable for evaluating LiDAR survey performance under varying conditions, including dense vegetation, steep slopes, and built structures.

In addition to the raw aerial LiDAR datasets, both control areas are supported by ground control points. Two of these 70 control points are already available for assessment and are located within the same areas as the two study areas used for ASL LiDAR data assessment. These ground control areas are used to evaluate vertical and planimetric accuracy by comparing the ALS dataset with TLS acquisitions conducted by MERMEC Engineering company.

In particular, the Northern control area benefits from two independent TLS surveys. The Laboratory of Geomatics at the University of Pavia, in collaboration with Microgeo , carried out TLS measurements in the test area, complemented by topographic and GNSS surveys, to achieve the highest possible survey precision. These TLS datasets serve as reference data for validating the ALS dataset, which is limited to the control areas.

2. Quality assessment of the raw LiDAR dataset

A key component of the quality assurance protocol involves the systematic evaluation of planimetric and altimetric consistency across overlapping LiDAR strips. This assessment is critical to ensure the accuracy of the aerial LiDAR-derived products, such as Digital Terrain Models (DTMs) and Digital Surface Models (DSMs). The entire procedure was developed in MATLAB (R2025a) using in-house algorithms, providing full customization of the workflows. This methodology enables visualization and examination of the entire LiDAR dataset, while all analyses are executed automatically, ensuring efficiency and reproducibility throughout the processing workflow. Furthermore, the developed algorithm is scalable, capable of processing large-scale aerial LiDAR surveys, enabling seamless application to the quality assessment of all aerial datasets involved in this project. The following sections detail the methodology used to evaluate the aerial dataset, focusing on the internal consistency of the flight strips and the planimetric and altimetric assessments in the two identified ground test areas.

2.1 Internal Quality Assessment of LiDAR Strips

The algorithm begins by loading the flight strips, which are divided into 1 km x 1 km tiles, and converts the coordinates from geographic (EPSG 6706) to cartographic (EPSG 7794). During this process, it also verifies that the point cloud generated from each tile contains enough points. The generated tiles inevitably produce marginal blocks along the boundaries of the surveyed area due to the irregular shape. In these perimeter zones, the overlap between the grid and the point cloud is minimal, resulting in tiles with very few points (fewer than 3). Since such a limited number of points does not allow for reliable processing, these perimeter tiles are identified using a predefined threshold (equal to a minimum of 3 points) and automatically excluded from subsequent processing stages. Managing and loading point clouds in a MATLAB environment is also not straightforward or fast. Therefore, for each individual file, all useful attributes (X, Y, Z, intensity, return number, number of returns, scan direction flag, edge of flight line, classification, scan angle rank, user data, point source ID) are extracted, and each tile is transformed into a more manageable tabular format.

Point clouds acquired via Airborne Laser Scanning (ALS) inherently contain outliers, either above or below the true surface, caused by atmospheric effects, airborne objects, sensor noise, or multipath reflections. To prevent these points from affecting subsequent analyses, a robust statistical filtering algorithm is applied across all dataset files, ensuring reliable and accurate results.

The cleaned point clouds are used to extract convex polygons for each tile. Polygons belonging to the same flight strip are merged, and overlaps between adjacent strips are determined by polygon intersections. These overlap regions are central to the analysis and are represented by densified polygons to ensure accurate spatial representation. For each region, a principal axis is estimated via PCA, along which equidistant points are generated, maintaining a 200 m buffer from the edges. Orthogonal lines are constructed at each point, and the midpoint of the intersections with the polygon defines the local center. Points are then interpolated using a spline, producing a continuous axis, along which control areas are sampled at 1000 m intervals. Unit normal vectors to the curve define the transverse orientation of each area, which is then centered on the midpoint, with a minimum distance of 200 m from polygon edges to avoid boundary effects. The resulting coordinates, normals, and strip metadata constitute the final set of control areas.

Within each control area, points from both overlapping strips are extracted. The clouds are translated to a common centroid and aligned via spatial correlation to identify point-to-point correspondences. Differences are computed in planimetry and elevation, and robust statistics are used to quantify alignment and quality. Vertical sections along east–west and north–south directions visualize local misalignments or deformations. All results per area are summarized in tables, providing a complete overview of displacements between adjacent strips.

Point cloud density is also evaluated. Tile polygons are combined to define the full block, which is overlaid with a 100 m × 100 m grid. For each cell, the area overlapping the tile polygon is calculated, and the point count is divided by this effective area to yield the true density. Repeating this for all tiles produces a raster describing spatial density across the entire dataset.

2.2 Plano-altimetric assessments in the ground control area

In the initial phase of the project, two out of the planned 70 control areas were made available, corresponding to the test sites for the airborne LiDAR data. These control areas serve as independent references and ground truth, and are crucial for validating the dataset's absolute positional accuracy. Their use ensures that the point cloud has been rigorously georeferenced within the project's coordinate system. Furthermore, the comparison between airborne data and high-precision terrestrial topographic surveys enables the exclusion of potential systematic errors (biases), GNSS/IMU trajectory deviations, or instrumental misalignments (boresight misalignment), thereby certifying the geometric reliability of the entire acquisition process. Within each control area, a TLS survey is conducted in open spaces selected to include significant vertical features, such as building facades, to assess the planimetric accuracy of the ALS data. The TLS survey sites were identified in urban areas with buildings

https://doi.org/10.5194/isprs-archives-XLIX-B2-2026-125-2026 | © Author(s) 2026. CC BY 4.0 License.

whose façades are suitable for planimetric comparison. These areas were specifically chosen because, in a subsequent phase of the project, a GNSS point acquisition technique using a Mobile Mapping Vehicle (MMV) will be implemented. This approach will enable an integrated dataset, facilitating comparison of data obtained through different surveying methodologies.

Given that the ALS data covers a very large area, the dataset is divided into thousands of files, organized into 1 km × 1 km tiles. To avoid inefficient searches through many files in the main code, a dedicated preprocessing module was developed. This module automatically identifies the ALS tiles that intersect the area covered by the TLS survey. To this end, the boundary of the area acquired with TLS is first generated, and then a spatial intersection analysis is performed with each individual ALS tile, identifying only the files that fall within the area of interest. In this way, the subsequent processing is limited to only the ALS point clouds relevant to the TLS survey.

The altimetric verification is performed using GNSS checkpoints. For each checkpoint, a portion of the TLS point cloud within a 1-meter radius of the checkpoint is selected, and a robust plane is estimated to represent the local surface. Subsequently, the ALS points that fall within the same 1-meter radius from the checkpoint are extracted, and the point-to-plane distance relative to the plane estimated by the TLS is calculated. The distances obtained are then analysed using robust statistical methods to assess the altimetric discrepancies between the two datasets. To ensure the reliability of the comparison, for each extracted plane, it is also verified that the point density exceeds a minimum threshold, defined differently for ALS and TLS data. This control ensures that comparisons are performed on surfaces that are sufficiently sampled and therefore statistically representative, reducing the risk of errors from insufficient sampling density.

The planimetric verification is more complex than the altimetric verification because it requires analysis of building facades in both the ALS and TLS point clouds. Extracting facades from the ALS point cloud is particularly challenging due to the predominantly nadir-viewing geometry, which results in low point density on vertical surfaces. Given that these checks must be performed across approximately 70 control areas, an automated procedure for facade extraction was developed and subsequently visually verified by an operator. The identification of facades is based on the analysis of the eigenfeatures of the local geometry of the point cloud. In particular, the characteristics of planarity, verticality, and linearity are used to identify vertical planar surfaces and to exclude linear elements, such as poles or other structures that do not belong to the facades. For each extracted facade, a robust plane is estimated to remove distracting elements (e.g., gutters, windowsills, railings, or balconies) and retain only the points that represent the wall surface. Starting from the facade identified in the TLS point cloud, a bounding box with a 25 cm margin is generated, and the corresponding ALS points are selected within it. A robust plane is also established on these points to ensure that the comparison is performed exclusively on the vertical surface. The plane derived from the TLS data is used as a reference; the ALS points are projected onto it, and the differences in the East and North components are calculated. The planimetric distance is then determined using the Pythagorean theorem and synthesized with robust statistical methods to assess planimetric consistency between the ALS and TLS datasets.

3. Results and discussion

The project is ongoing, and full data collection across the entire dataset has not yet been completed. For the purposes of this study, we focus on two preliminary test areas selected to evaluate raw LiDAR data, validate verification procedures, and assess LiDAR sensor performance. The results presented here, therefore, represent only this initial subset of the project.

In this section, the results for the two available control areas are presented. These areas serve as a reference for assessing both the planimetric and altimetric accuracy of the LiDAR data, illustrating the alignment between adjacent strips and correspondence with TLS measurements, thus providing a comprehensive overview of the dataset’s geometric quality.

The Northern control area comprises 51 overlapping LiDAR flight strips, stored in LAS format and tiled into 1km x 1km tiles, resulting in 8,990 files totalling 1.89 TB. The central (Lazio) control area consists of 59 overlapping LiDAR flight strips, stored in compressed LAZ format and tiled into 1km x 1km tiles, resulting in 11,465 files with a total data volume of 0.8 TB. The overlap of these strips ensures complete coverage and redundancy, which is essential for assessing the consistency and quality of the LiDAR point clouds across different acquisition conditions.

3.1 Observed internal consistency of LiDAR strips

The internal geometric consistency of the LiDAR dataset was evaluated by analysing the overlapping regions between adjacent flight strips. The automatically generated check areas described in Section 3 were used to extract corresponding points from the two strips and to compute the planimetric and altimetric differences.

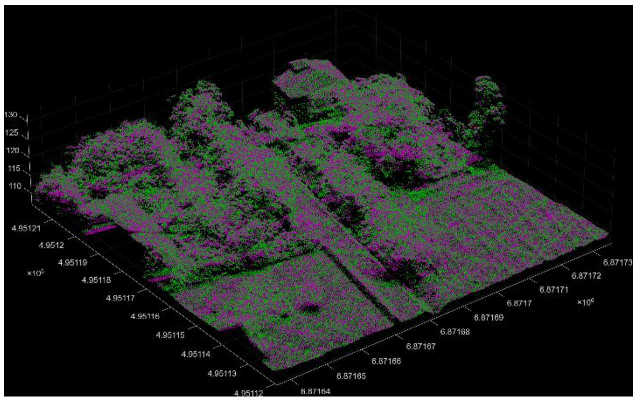

Figure 2. Example of one of the 3,500 check areas in the Northern test area.

Within the two zones, check areas were automatically created in the overlap regions between adjacent strips. An example from the Northern control zone is shown in Figure 2. There are 70 overlapping regions, each containing 50 check areas spaced 1,000 m apart, for a total of 3,500 check areas. For each check area, LiDAR points from both strips were extracted and stored in an organized structure.

For each check area, the two LiDAR point clouds from the overlapping strips were first co-registered to identify corresponding points between the datasets. The registration procedure returns the indices of the matched points in the two strips, establishing a point-to-point correspondence between the datasets. Using these indices, the geometric differences between each pair of corresponding points were computed. In particular, the horizontal displacement and the elevation differences were calculated for all matched points within each check area.

The resulting distances were then analysed and visualised as a graphical representation for each component (East, North, Height), with each check area represented by a different colour, allowing an immediate assessment of the internal geometric consistency between the overlapping strips. For the purposes of this study and to maintain clarity in the presentation of results, only the raster representing the elevation component is shown. The other raster layers in the dataset are omitted here for brevity, as the elevation raster sufficiently illustrates the key aspects of the analysis.

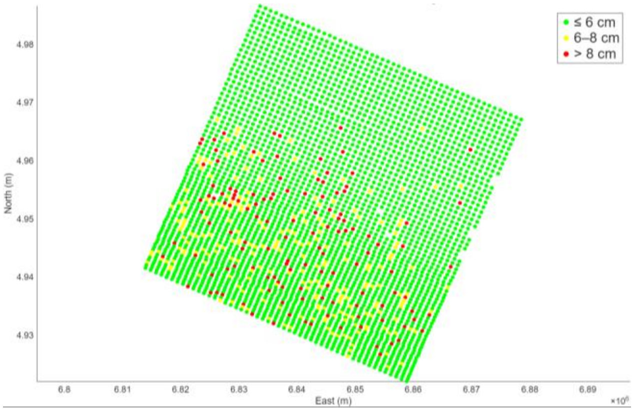

Figure 3. Spatial variations in the vertical component for the Northern control area are represented using three colour classes, highlighting areas with low, medium, and high RMSE values.

Figure 3 shows the distribution of elevation differences across the two check areas relative to the proposed technical specification. Most points fall below the threshold of 6 cm (green), a smaller portion lies between 6 and 8 cm (yellow), and only a very limited fraction exceeds the specification limits (red). As described in Section 2, the Northern test area was selected so that part of the study area encompasses the Apennines, a topographically challenging region characterized by mountainous terrain and dense vegetation. Nearly all red points, and some yellow points, are in these vegetated areas. Since the two strips were acquired at different times and from distinct viewpoints, corresponding points in vegetated areas do not necessarily represent the same leaf or branch in both strips. This depends on both the aircraft flight path and the LiDAR sensor’s ability to penetrate the vegetation. This vegetation is currently under investigation. We are evaluating an automatic algorithm to remove vegetation from individual check areas, so that comparisons are performed only on solid structures such as roofs, building facades, the ground, and other non-vegetated elements. To further illustrate that these differences are influenced by vegetation, Figures 4 and 5 show two sections of one of the check areas (highlighted in red). In particular, the cross-section plots refer to the check areas associated with strip number 65 and check area number 30. Points from the two strips are displayed in distinct colours (magenta and green), and no deviations are observed, confirming that the differences are primarily due to vegetation.

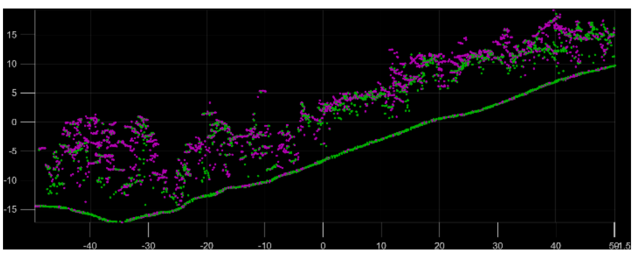

Figure 4. East-West cross-section for the check area 65-30 showing the points from the two adjacent LiDAR strips in magenta and green.

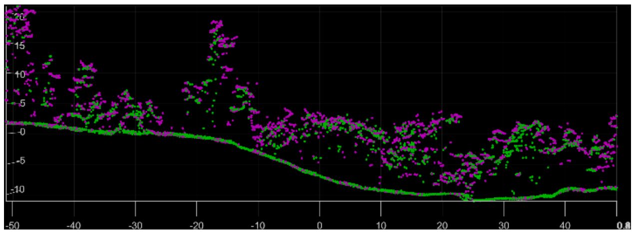

Figure 5. North-South cross-section for the check area 65-30 showing the points from the two adjacent LiDAR strips in magenta and green.

When considering both sections and focusing exclusively on the ground surface, no discrepancies are observed, and the profiles from the two flight strips align closely. Vegetation, however, plays a critical role in these observations: because the same tree is captured from two distinct viewpoints, it cannot be assumed that corresponding points correspond to the same part of the tree. This explains why such phenomena are occasionally observed in certain portions of the test block dataset.

Component	Reference value (cm)	Median RMSE (cm)
East	15 (2D)	7.1
North		7.4
Vertical	8	2.6

Table 1. Comparison between the reference values and the median RMSE for each component. The reported values refer to the 3,500 check areas analysed in the Northern test area, corresponding to 70 overlapping adjacent strip areas and covering a total of 8,990 tiles.

For each check area, a comprehensive statistical characterization was performed, calculating the mean, standard deviation, RMSE, and median, along with robust estimators for both standard deviation and RMSE. As summarized in Table 1, the global accuracy was evaluated using the reference RMSE and the median robust RMSE. The vertical component yielded a robust RMSE of approximately 3 cm, significantly below the 8 cm threshold defined in the technical specifications. The planimetric components, while remaining largely within the 15 cm allowable limit, showed an error of approximately 7 cm for both components. This trend is primarily attributable to dense vegetation in mountainous terrain; in these areas, LiDAR returns from overlapping flight strips may not coincide with the same ground or canopy features. Such planimetric discrepancies are particularly pronounced in individual tree structures, where the lack of precise geometric correspondence between strips can introduce minor apparent offsets.

In the Central test area, a systematic validation protocol was implemented, resulting in the automatic generation of 1,639 check areas positioned within the overlap regions of 59 adjacent flight strips. To ensure statistical significance and spatial homogeneity across the survey extent, approximately 28 check areas were distributed within each overlapping zone. Following the methodology established for the Northern control site, LiDAR point cloud segments from corresponding strip pairs were extracted and co-registered. This process facilitated a rigorous point-to-point correspondence analysis, enabling the precise computation of both horizontal and vertical discrepancies across all matched coordinates.

The spatial distribution of these discrepancies was categorized and visualized to assess localized performance. As illustrated in the North component raster (Figure 6), the vast majority of check areas (indicated in green) fall well below the stringent internal technical threshold of 6 cm. A secondary fraction of the samples exhibits moderate deviations of 6-8 cm (yellow), while only a negligible number of points, localized to specific environmental contexts, completely exceed the project specifications (red).

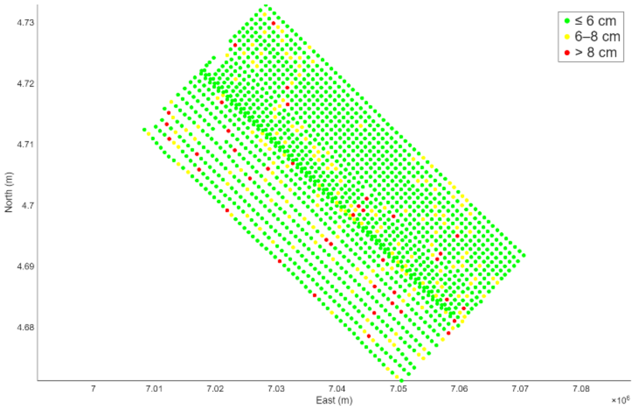

Figure 6. Spatial variations in the vertical component for the Central test area are represented using three color classes, highlighting areas with low, medium, and high RMSE values.

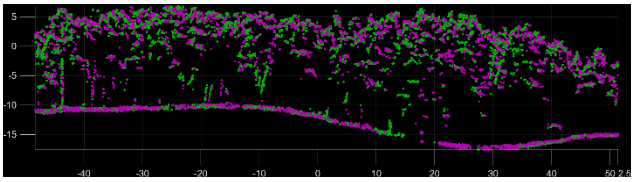

Figure 7. North-South cross-section for the check area 23-49 showing the points from the two adjacent LiDAR strips in magenta and green.

Quantitative assessment of the statistical indices, summarized in Table 2, confirms a high degree of internal consistency within the dataset. The vertical component yielded a robust RMSE of approximately 5 cm, remaining comfortably within the 8 cm allowable limit. Similarly, the planimetric components demonstrated high stability, with robust RMSE values of approximately 6.4 cm for the East and 6.5 cm for the North components. The combined planimetric RMSE of 9 cm remains significantly below the maximum permissible threshold of 15 cm defined in the technical offer.

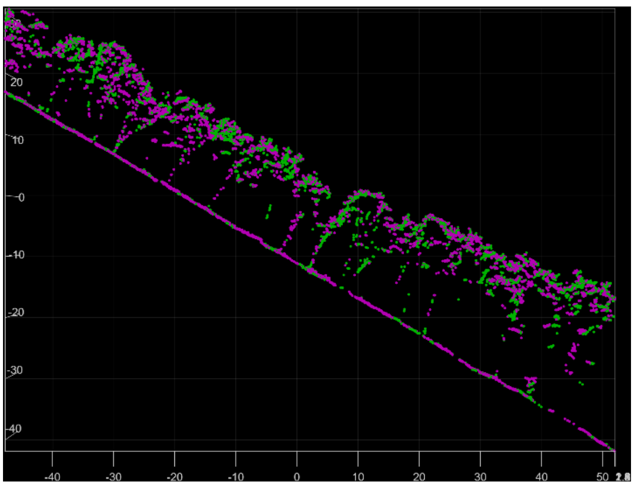

Figure 8. East-West cross-section for the check area 23-49 showing the points from the two adjacent LiDAR strips in magenta and green.

Although the Central area has more regular topography and lower vegetation density than the Northern test site, localized planimetric deviations persist in vegetated sections. This phenomenon is empirically supported by the cross-sectional analysis of Strip 23 (Check Area 49; Figures 7 and 8), which reveals that, while ground-level profiles from overlapping strips align nearly perfectly, the canopy structure introduces geometric noise. These discrepancies arise from the sensor's varying look angles, which capture distinct portions of the foliage from different perspectives. Consequently, advanced vegetation filtering algorithms are currently being investigated to mitigate these perspective-induced offsets and further refine the planimetric consistency of the final point cloud.

Component	Reference value (cm)	Median RMSE (cm)
East	15 (2D)	6.4
North		6.5
Vertical	8	4.9

Table 2. Comparison between the reference values and the median RMSE for each component. The reported values refer to the 1,639 check areas analysed in the Central test area, corresponding to 59 overlapping adjacent strip areas and covering a total of 11,465 tiles.

3.2 Ground truth and TLS validation

To assess the accuracy of the aerial LiDAR acquisitions, ground control areas were established in both study areas using TLS surveys. These control areas provided high-precision reference data, enabling a detailed evaluation of vertical and planimetric discrepancies of the ALS dataset.
The TLS LiDAR point clouds for both ground control areas have an average density of approximately 4,000 points/m^2.
The Northern control area was surveyed through two independent TLS campaigns. In conjunction with the TLS survey of the Northern test area carried out by MERMEC Engineering for acquiring the 70 ground control areas distributed across the Italian territory, the Geomatics Laboratory of the University of Pavia conducted, on the same day, a high-precision survey integrating GNSS, Total Station (TTS), and TLS techniques.
Notably, the Northern test site was the only area subjected to this redundant surveying approach. By employing two independent teams and different topographic instruments (GNSS, TTS, and TLS) on the same day, a robust cross-validation framework was established. This enables an empirical assessment of the acquisition protocols used by MERMEC Engineering, ensuring that the TLS-derived ground control areas across the entire Italian territory meet the required accuracy and quality standards. The topographic infrastructure built a redundant reference network for LiDAR validation, ensuring stability and accuracy. A multi-sensor approach used a Leica MS60 Total Station for control points via inter-visible stations. Static GNSS data at key points provided an absolute coordinate system to align terrestrial LiDAR with aerial data. The primary terrestrial laser scanning (TLS) campaign, conducted with a RIEGL VZ-600i, prioritized acquiring dense vertical geometries, such as building facades, to provide unambiguous features for planimetric accuracy assessments. To minimize registration drift and ensure sub-centimeter consistency, the TLS stations were directly integrated into the topographic network; physical markers on tripods served as common reference targets, tying the scan data directly to the GNSS-supported control points.

Figure 9. Top view of the LiDAR point cloud acquired through Riegl VZ-600i by the Laboratory of Geomatics.

In parallel, an independent validation survey was performed by MERMEC Engineering using a Leica RTC360 laser scanner. This secondary acquisition was georeferenced using a GNSS NRTK (Network Real-Time Kinematic) framework with Leica GS16 and GS18 I receivers. The coexistence of these two distinct instrumental setups, the RIEGL system integrated into a static topographic network and the Leica system supported by NRTK positioning, allowed for a rigorous cross-comparison of the acquisition protocols and a more comprehensive validation of the ground control areas. This rigorous alignment process resulted in a high-fidelity reference point cloud (Figure 9), which served as the "ground truth" for evaluating the aerial survey. In the Northern control area, this benchmark enabled a direct intercomparison between independent TLS datasets, focusing primarily on the vertical component to isolate and quantify potential systematic biases in the acquisition chain.

To evaluate inter-dataset consistency, a plane-fitting approach was applied to 10 control points from the topographic network, characterized by stable, unobstructed planar surfaces, such as road edges. For each reference point, LiDAR returns were extracted within a 1-meter radius from both TLS datasets. A robust plane was then fitted to the point cloud acquired by the Geomatics Laboratory, serving as a high-precision reference. Subsequently, the orthogonal distances of the corresponding points from the second TLS dataset were computed relative to these reference planes. The results yielded a mean deviation of approximately 1.9 cm across the distributed sample points, indicating a high degree of vertical coherence between the two independent acquisitions. While the vertical alignment showed strong agreement, a direct planimetric consistency assessment between the two independent TLS surveys could not be performed. This limitation was due to the absence of well-defined vertical surfaces within the overlapping acquisition areas, which prevented the extraction of sufficiently reliable point cloud segments for a robust horizontal comparison.

Once the reliability and internal consistency of the TLS reference datasets were established, the validated terrestrial point cloud was employed as a high-precision benchmark to evaluate the absolute accuracy of the Aerial Laser Scanning (ALS) data.

3.3 Plano-altimetric accuracy in the ground control areas

The absolute metric accuracy of the Aerial Laser Scanning (ALS) data was rigorously evaluated using a dual-component validation framework, with high-precision Terrestrial Laser Scanning (TLS) datasets as the primary benchmark. This methodology distinguishes between vertical and planimetric assessments to account for the different geometric sensitivities of LiDAR sensors relative to topography and the built environment. The vertical validation focused on characterizing stable, horizontal surfaces, which provide the most reliable basis for elevation checks. A series of GNSS-referenced checkpoints was strategically distributed across road pavements and unobstructed ground areas to provide a geodetic reference frame. At each checkpoint, a robust plane-fitting algorithm was applied to the TLS point cloud within a 1-meter radius, using least-squares estimation to define a local "ground truth" surface, thereby minimizing the influence of sensor noise or micro-topographic irregularities. The corresponding ALS points within these defined radii were extracted, and their orthogonal distances to the reference TLS planes were computed.

Component	Reference value (cm)	Median RMSE (cm)	
		UNIPV	MERMEC
Horizontal	15	9.5	7.9
Vertical	8	4.4	5.5

Table 3. Summary of accuracy obtained for the Northern test area using both UNIPV and MERMEC TLS data.

Component	Reference value (cm)	Median RMSE (cm)
Horizontal	15	8.1
Vertical	8	7.7

Table 4. Summary of accuracy obtained for the Central test area using MERMEC TLS data.

As summarized in Table 3, the vertical assessment in the Northern test area yielded a median RMSE of 4.4 cm for the UNIPV reference and 5.5 cm for the MERMEC survey. Similarly, in the Central test area (Table 4), the vertical comparison between the MERMEC TLS and ALS data yielded a robust RMSE of 7.7 cm. This value confirms that the elevation consistency across both sites remains within the project's 8 cm technical threshold, even when accounting for the increased topographic complexity of the central survey area.

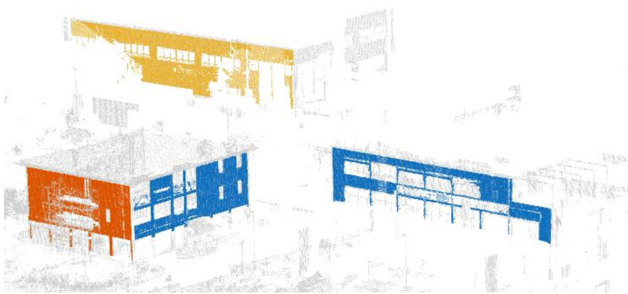

Figure 10. Example of automatically extracted building facades in the Northern ground control area. The extracted facades are highlighted in different colours, while the original TLS point cloud is displayed in grey.

Subsequently, the planimetric validation was addressed through a more complex procedure, as horizontal displacements are inherently difficult to isolate on flat or gently sloping ground. Consequently, the assessment relied on identifying vertical structural elements, specifically building facades, which provide unambiguous geometric constraints for X-Y coordinate verification. An eigenfeature-based automated algorithm was employed to segment these vertical surfaces from the dense TLS point clouds (Figure 10). To ensure the geometric integrity of the resulting reference planes, a robust estimation filter was implemented to exclude architectural protrusions and "noise" (e.g., windows, shutters, balconies, and gutters), thereby isolating the primary structural facade.

The planimetric accuracy was then quantified by measuring the horizontal displacement of the ALS points relative to these refined vertical TLS planes. In the Northern area, 12 distinct facades were analyzed for each survey. Despite the lack of shared surfaces between the two independent terrestrial acquisitions due to differing sensor viewpoints, the results were highly consistent. The median RMSE was recorded at 9.5 cm for the UNIPV reference and 7.9 cm for the MERMEC reference. A similar procedure in the Central area, using seven automatically extracted facades, yielded a planimetric RMSE of 8.1 cm. These findings, all significantly below the 15 cm allowable limit, verify the absence of systematic horizontal shifts and confirm the high metric reliability of the ALS dataset for large-scale mapping applications.

4. Conclusion

Implementing a fully automated, comprehensive quality assurance protocol is essential to ensure the reliability and usability of nationwide LiDAR datasets. The methodologies presented in this study, including systematic congruence analysis of overlapping flight strips and rigorous assessment of planimetric and altimetric accuracy using independent TLS surveys, demonstrate that high standards of geometric consistency and spatial accuracy can be achieved even at the national scale.

Automation of the validation workflow plays a crucial role in this context. It enables efficient processing of extremely large datasets while ensuring reproducibility, objectivity, and consistency in the quality-control procedures. The integration of multiple complementary analyses, including strip overlap evaluation, using check areas equidistantly distributed within overlapping areas, and independent TLS validation, provides a robust and comprehensive framework for assessing ALS data quality. The influence of vegetation on the evaluation of contiguous strips remains under investigation.

The authors are currently developing an automatic algorithm to remove vegetation from individual check areas, allowing comparisons to focus exclusively on solid structures such as roofs, building facades, ground surfaces, and other non-vegetated elements. Implementing this approach will improve the assessment of internal consistency between adjacent strips, providing more reliable insights into the geometric accuracy of the LiDAR dataset. Despite the influence of vegetation, the measured values remain well within the thresholds defined by the technical specifications.

The results confirm the high geometric reliability of the ALS acquisitions. The analysis of overlapping strips shows a strong internal consistency of the dataset, while the comparison with high-density TLS reference data demonstrates that the achieved accuracies meet the requirements defined in the technical specifications. Localized discrepancies observed in some areas are primarily attributable to vegetation effects and differences in observation geometry between acquisition strips, rather than to systematic geometric errors. Overall, the proposed validation framework provides a reliable basis for evaluating both the relative and absolute accuracy of large-scale ALS datasets. Furthermore, the methodology presented in this work can serve as a reference for future national-scale LiDAR acquisition campaigns, contributing to the development of standardized and reproducible quality-assessment procedures for geospatial data.

References

Brown, R., Hartzell, P., & Glennie, C., 2020. Evaluation of SPL100 Single Photon Lidar Data. *Remote Sensing*, *12*(4), 722. https://doi.org/10.3390/rs12040722.

Franzini, M., Casella, V.M. and Monti, B., 2023. Assessment of Leica CityMapper-2 LiDAR data within Milan’s Digital Twin Project. Remote Sensing, 15(21), p.5263. https://www.mdpi.com/2072-4292/15/21/5263.

Hopfstock, A., Knöfel, P. and Lindl, F., 2022. Digital Twin Germany–a digital replica for simulation and analysis build on geospatial data. *Abstracts of the ICA*, 5, 1-2. https://doi.org/10.5194/ica-abs-5-119-2022.

Institut national de l’information géographique et forestière (IGN), 2026. *Programme LiDAR HD: vers une nouvelle cartographie 3D du territoire*. https://geoservices.ign.fr/lidarhd (12 February 2026).

Leica Geosystems AG, 2019. *Leica TerrainMapper: Airborne LiDAR Mapping System Product Specifications*.

RIEGL Laser Measurement Systems GmbH, 2026a. *RIEGL VQ-1460: Waveform Processing Airborne LiDAR Scanning System*. https://www.riegl.com/de-oesterreich/products/detail/riegl-vq-1460 (14 March 2026).

RIEGL Laser Measurement Systems GmbH, 2026b. *RIEGL VQ-780 II-S: Waveform Processing Airborne Laser Scanner*. https://www.riegl.com/en-austria/products/detail/riegl-vq-780-ii-s (18 March 2026).

Scott, C.P., Beckley, M., Phan, M., Zawacki, E., Crosby, C., Nandigam, V. and Arrowsmith, R., 2022. Statewide USGS 3DEP lidar topographic differencing applied to Indiana, USA. *Remote Sensing*, 14(4), 847. https://doi.org/10.3390/rs14040847.